Interaction of Magnesium and Inorganic Phosphate with Calcium-Deprived Sarcoplasmic Reticulum Adenosinetriphosphatase As Reflected by Organic Solvent Induced Perturbation

Ph. Champeil,* F. Guillain, C. Vénien, and M. P. Gingold

Groupe de Biophysique des Systèmes Membranaires, Service de Biophysique, Département de Biologie, Centre d'Etudes Nucléaires de Saclay, 91191 Gif-sur-Yvette Cedex, France
Received February 22, 1984; Revised Manuscript Received June 28, 1984

ABSTRACT: The mechanism of sarcoplasmic reticulum (SR) ATPase Mg^{2+}-dependent phosphorylation from P_i was investigated in the presence of 15% v/v dimethyl sulfoxide at pH 6, 20 °C, and in the absence of potassium. Measurements of intrinsic fluorescence changes and of ^{32}P-labeled phosphoprotein (*E-P) were in agreement, both at equilibrium and in transient situations. We found that the amount of phosphoenzyme present and its rate of formation depended solely on the concentration of the ($Mg{\cdot}P_i$) complex. Up to 6 nmol of phosphate/mg of protein was covalently bound to the enzyme, implying almost complete phosphorylation. Oxygen exchange experiments were also performed in order to allow calculation of the absolute rate constant of *E-P hydrolysis to the noncovalent complex (0.8–1.0 s^{-1}), which differs from the observed rate of enzyme dephosphorylation (0.3–0.5 s^{-1}); in addition, they allowed calculation of the bimolecular rate constant of substrate binding (2–2.4 M^{-1} s^{-1}). The results demonstrate that in the presence of dimethyl sulfoxide, phosphorylation occurs by the following simple mechanism: relatively slow binding of the neutral substrate ($Mg{\cdot}P_i$), with poor affinity, followed by a thermodynamically favorable formation of the covalent bond between phosphate and the possibly hydrophobic active site. The interaction between magnesium and calcium-deprived SR vesicles was studied in the presence of 0–20% v/v dimethyl sulfoxide (or 0–30% v/v glycerol) at pH 7 and 20 °C. The presence of either solvent led to the disappearance of the two typical pH-dependent effects we previously characterized for magnesium: loss of the Mg^{2+}-induced spectral shift of tryptophan fluorescence emission and loss of the biphasic pattern displayed by the intrinsic fluorescence rise after addition of calcium to Ca^{2+}-deprived Mg^{2+}-preincubated vesicles. In the absence of solvent, the interaction of magnesium with the calcium-deprived ATPase was also characterized from the point of view of phosphoenzyme formation from ATP or P_i at pH 7 in the absence of potassium: we found that calcium-independent phosphorylation was slower when phosphate was added to SR vesicles preincubated with magnesium than when magnesium was added to vesicles preincubated with phosphate, suggesting that preincubation with magnesium had depleted the phosphate-reactive conformation of the ATPase. A simple reaction scheme for phosphoenzyme formation is described: it implies that the ($Mg{\cdot}P_i$) complex is a substrate for this reaction, whereas the Mg^{2+} itself acts as a pH-dependent, dimethyl sulfoxide sensitive inhibitor of full enzyme phosphorylation. The rate of the transition from the Ca^{2+}-deprived ATPase conformation to the Ca^{2+}-saturated conformation was also shown to be slowed down in the presence of dimethyl sulfoxide or glycerol.

Soon after the discovery that calcium uptake by sarcoplasmic reticulum vesicles was reversibly coupled to ATP[1] hydrolysis (Makinose & Hasselbach, 1971), it was observed that phosphoprotein formation from P_i, the first step in the calcium release coupled ATP synthesis reaction, could also be obtained in the absence of a calcium concentration gradient across the membrane, provided the external high-affinity calcium binding sites were not occupied by calcium (Masuda & de Meis, 1973; Kanazawa & Boyer, 1973; Knowles & Racker, 1975; Beil et al., 1977). Such phosphoprotein formation from P_i was found to be magnesium dependent. After careful examination of several possible schemes, reaction Scheme I, involving the random binding of magnesium and P_i suggested earlier for

Scheme I

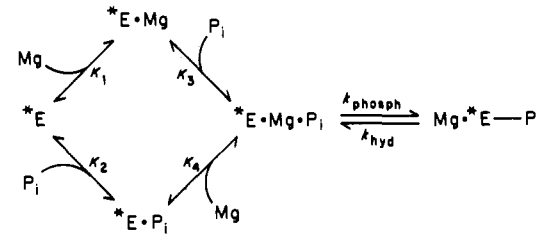

Na^+–K^+ ATPase, was proposed in order to account for equilibrium measurements of SR phosphorylation from P_i (Kuriki et al., 1976; Kolassa et al., 1979; Punzengruber et al., 1978; Epstein et al., 1980; Lacapère et al., 1981; Martin & Tanford, 1981; Watanabe et al., 1981; de Meis et al., 1982).

It was subsequently established that very high concentrations of magnesium inhibited phosphoenzyme formation from P_i (Martin & Tanford, 1981; Inesi et al., 1984), an observation that had in fact been made earlier but had been ignored (Kanazawa, 1975). This inhibition was accounted for by assuming that magnesium was driving the enzyme away from

[1] Abbreviations: ATPase, adenosinetriphosphatase; SR, sarcoplasmic reticulum; Mes, 2-(*N*-morpholino)ethanesulfonic acid; Mops, 4-morpholinepropanesulfonic acid; EGTA, ethylene glycol bis(β-aminoethyl ether)-*N*,*N*,*N*′,*N*′-tetraacetic acid; EDTA, ethylenediaminetetraacetic acid; Tris, tris(hydroxymethyl)aminomethane; ATP, adenosine triphosphate; TNP-ATP, 2′,3′-*O*-(2,4,6-trinitrocyclohexadienylene)-adenosine triphosphate; PCA, perchloric acid; $\Delta F/F$, relative fluorescence change; k_{obsd}, observed rate constant; Me_2SO, dimethyl sulfoxide.

0006-2960/85/0424-0069$01.50/0

what is known as the *E (or E_2) phosphate-reactive conformation (Martin & Tanford, 1981; Loomis et al., 1982). A similar suggestion was deduced from the results of our study of the interaction of magnesium with Ca^{2+}-deprived SR ATPase, in which we stressed the pH dependence of this interaction (Guillain et al., 1982). More recently, completely independent structural evidence supporting the view that the *E conformation is depleted in the presence not only of calcium but also of magnesium alone came from Ikemoto's laboratory, where the second trypsin cleavage site was found to shift to different positions in the presence or absence of calcium or magnesium (Marczek et al., 1983).

In 1980, de Meis and co-workers demonstrated several remarkable effects of certain solvents on SR ATPase phosphorylation from P_i: this enzyme's apparent affinities for phosphate and magnesium were enhanced by 2 or 3 orders of magnitude by adding up to 40% dimethyl sulfoxide (Me_2SO), and phosphoenzyme formation became pH- and temperature-independent (de Meis et al., 1980). This paper extends these observations and takes advantage of dimethyl sulfoxide and glycerol perturbation to acquire further information about the interaction of Ca^{2+}-ATPase with inorganic phosphate and magnesium.

We reinvestigated the mechanism of magnesium-dependent phosphoenzyme formation from P_i in the presence of 15% Me_2SO at pH 6. Phosphoenzyme was determined either by measuring [^{32}P]phosphate incorporation or by recording the changes in intrinsic fluorescence induced by *E-P formation (Lacapère et al., 1981); we also measured, with [^{18}O]P_i, the water-medium phosphate exchange resulting from dynamic reversal of enzyme phosphorylation (Boyer et al., 1977). The data for all three techniques were consistent. In view of these results, we suggest that in the presence of Me_2SO there is no reason to assume that the mechanism involved in phosphorylation from P_i is more complicated than the one shown in Scheme II, in which the ($Mg{\cdot}P_i$) complex is simply the true substrate.

Scheme II

$$*E + Mg{\cdot}P_i \rightleftharpoons *E{\cdot}Mg{\cdot}P_i \rightleftharpoons Mg{\cdot}*E\text{-}P$$

Turning to the ATPase interaction with magnesium alone, we found that besides the change in water activity (Dupont & Pougeois, 1983) an essential difference between the situation observed in the presence of Me_2SO and that commonly obtained in the absence of solvent resided in the less efficient Mg^{2+}-induced depletion of the phosphate-reactive ATPase conformation, as revealed by fluorescence measurements performed as previously described (Guillain et al., 1982; Champeil et al., 1983). Conversely, we showed that the effect of such inhibition, which even occurs with moderate magnesium concentrations, must definitely be taken into account when describing the mechanism of *E-P formation under standard conditions (Scheme III).

Experimental Procedures

Fragmented sarcoplasmic reticulum was prepared and tested as already described (Champeil et al., 1978), with minor modifications: in particular, long centrifugation runs at a moderate speed were preferred to shorter runs at a higher speed, in order to avoid possible pressure-induced damage (Champeil et al., 1981). Fluorescence equilibrium and stopped-flow measurements were performed as described in Guillain et al. (1980) and Champeil et al. (1983). Inorganic phosphate was added as Tris salt. SR vesicle phosphorylation

Scheme III

$$E?Mg \underset{pH\ Me_2SO}{\overset{Mg}{\rightleftharpoons}} *E + Mg{\cdot}P_i \rightleftharpoons *E{\cdot}Mg{\cdot}P_i \rightleftharpoons Mg{\cdot}*E\text{—}P$$

from P_i was chemically determined in media containing [^{32}P]phosphate, as in Lacapère et al. (1981). To reduced background noise due to nonspecific binding, protein concentrations of 1–10 mg/mL were used (the EGTA concentration was accordingly raised to 5 or 10 mM), and protein-loaded filters were extensively rinsed. The multimixing experiments were performed with a Dionex (Durrum) D133 apparatus, and phosphorylation was quenched by mixing the samples with an equal volume of 240 mM PCA + 30 mM P_i, before dilution with 120 mM PCA + 15 mM P_i and filtration.

For calculation of the free ionic concentrations in our media, the following constants (pH 6) were used (Guillain et al., 1980): [Mg·EGTA]/([Mg][EGTA]) = 3.3 M^{-1}; [Mg·EDTA]/([Mg][EDTA]) = 1.46 10^4 M^{-1}. The dissociation constant of the $Mg{\cdot}P_i$ complex at pH 6 was 80 mM in water, whether it was calculated from tables [as in Lacapere et al. (1981)] or measured from the H^+ released upon complex formation. In the presence of 15% Me_2SO, the measured dissociation constant shifted to 140 mM. However, in some of our experiments such as those illustrated in Figure 2, we did not take this small shift into account.

We measured the Ca·EGTA dissociation constant at pH 7 and 25–30 °C, in the absence or presence of 20% Me_2SO, by titrating the protons released upon complex formation (Dupont, 1982). In the absence of solvent, we determined a dissociation constant of 4×10^{-7} M, in agreement with Dupont's measurement at 20 °C and with our calculations based on Allen's absolute constant for the Ca + EGTA ⇌ Ca·EGTA equilibrium [see Guillain et al. (1980)]. Me_2SO at 20% v/v was found to have no effect on the dissociation constant.

All media were buffered at either pH 6 ± 0.1 or pH 7 ± 0.1 (20 ± 1 °C) and contained no potassium (for the ^{32}P experiments using high enzyme concentrations, SR vesicles were previously washed to remove the K^+ present in the storage medium). Me_2SO concentrations are expressed in percent of volume. All experiments were performed at 20 °C.

Oxygen experiments were carried out as described in McIntosh & Boyer (1983). The following formulas were used in the calculations (symbols are defined under Results):

$$P_c = (1/3)(4 - k_4/k_{av})$$

(k_4 and k_{av} are expressed in units of reciprocal time)

$$v_{ex,obsd} = 4k_{av}[P_i]/[\text{protein}]$$

[expressed as nmol/(mg min)]

$$\alpha = (4 - 4P_c)/(4 - 3P_c)$$

[cf. Hackney et al. (1980)].

Consider a P_i molecule covalently bound to the ATPase (*E-P). The rate at which the covalent bond will be broken and P_i released into the medium during a dephosphorylation experiment (k_{OFF}) is equal to the rate of transition from *E-P to $*E{\cdot}P_i$ (governed by k_{-2}, Scheme IV) multiplied by the probability that the P_i molecule is released rather than exchanged again (this probability is equal to $1 - P_c$). Therefore, $k_{OFF} = k_{-2}(1 - P_c)$.

Results

Equilibrium Measurements of P_i-Derived Phosphoenzyme

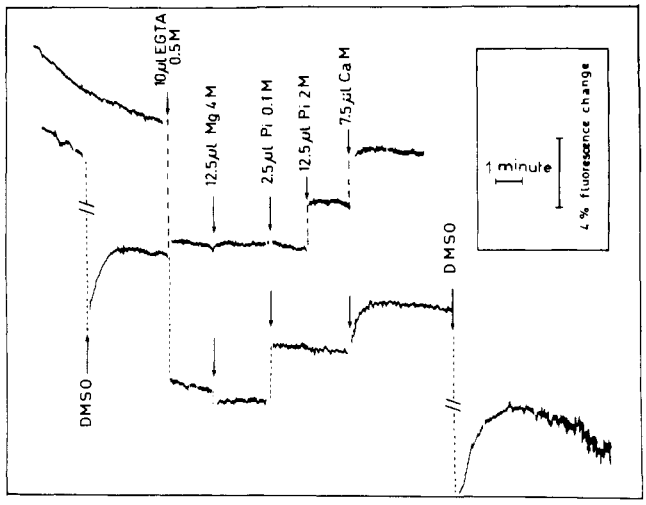

FIGURE 1: Ligand-induced intrinsic fluorescence changes in the absence (upper trace) or presence (lower trace) of Me_2SO. Vesicles (40–50 μg/mL) were suspended in 2.5 mL of buffer (150 mM Mes–Tris, pH 6, 20 °C). Lower trace shows the initial addition of Me_2SO at a final concentration of 15% v/v. The last addition of Me_2SO increased its concentration up to 40%. Excitation wavelength was 290 nm; emission wavelength was 320 nm for this recording.

in the Presence of Me_2SO at pH 6. Figure 1 shows how *E-P formation manifests itself on a recording of SR intrinsic fluorescence. The upper trace illustrates the standard pattern previously observed in a pH 6 medium without organic solvent (Lacapère et al., 1981), as follows: after SR vesicles were added to buffer in a fluorometer cuvette, chelation of calcium allowed intrinsic fluorescence to drop by a few percent [the so-called $E(Ca)_2 \rightarrow$ *E transition], and subsequent addition of 20 mM magnesium only enhanced fluorescence slightly [this effect of magnesium is pH dependent; see Guillain et al. (1982)]. Addition of 0.1 mM P_i was not sufficient to allow phosphoenzyme formation and, therefore, significant fluorescence enhancement, but further addition of 10 mM P_i fully demonstrated such formation (Lacapère et al., 1981). Addition of calcium restored the fluorescence level of the "$E(Ca)_2$" conformation.

In the experiment illustrated in the lower trace of Figure 1, 15% Me_2SO was added to SR ATPase; a large drop in fluorescence resulted from the dilution and sudden increase in temperature caused by the mixing of Me_2SO and buffer; upon temperature reequilibration of the cuvette, fluorescence was stabilized. Addition of EGTA revealed that the ATPase was still sensitive to calcium chelation. Subsequent addition of magnesium only resulted in dilution with no accompanying fluorescence enhancement (this finding will be more fully described below, see Figure 8). When 0.1 mM P_i was then added, fluorescence rose, a result consistent with the enhanced ATPase affinity for P_i; a further 10 mM P_i addition only produced a slight additional rise in the fluorescence level (not shown).

When calcium was added in the presence of 0.1 mM P_i, a return to the fluorescence level of the E conformation was observed, concomitantly with slow calcium-induced dephosphorylation. This fluorescence rise was even slower (not shown) in the presence of higher P_i concentrations, as previously observed and explained in the absence of Me_2SO (Guillain et al., 1981). When up to 40% additional Me_2SO was added, the fluorescence trace revealed, after temperature reequilibration, an increasing level of noise, and the ATPase in the cuvette was found to be highly aggregated. Optical

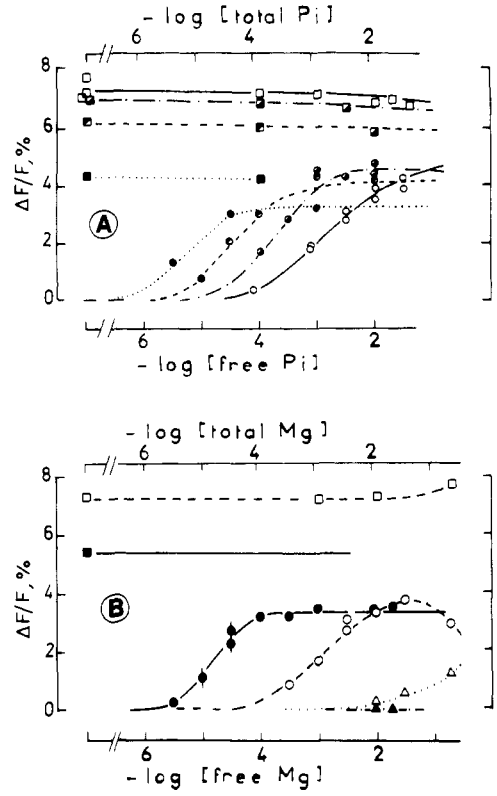

FIGURE 2: Titration of the ligand-induced intrinsic fluorescence changes without Me_2SO and in the presence of various amounts of Me_2SO. (A) A free Mg^{2+} concentration of 20 mM was kept constant in all media. Either varying concentrations of phosphate were added (circles) or calcium was added first (final pCa 3) and phosphate later (squares): (○, □) 0% Me_2SO; (bottom diagonal solid circle, bottom diagonal solid square) 8% Me_2SO; (top diagonal solid circle, top diagonal solid square) 15% Me_2SO; (●, ■) 24% Me_2SO. (B) Different concentrations of Mg were added to the Ca^{2+}-deprived enzyme (△, ▲). Then, either P_i was added up to a constant free concentration of 10 mM (circles) or calcium was added up to pCa 3 (squares). The lowest Mg concentrations were established with an Mg-EDTA buffer. Excitation wavelength was 290 nm; emission wavelength was 330 nm. Buffer contained 2 mM EGTA and 115–150 mM Mes–Tris (pH 6, 20 °C): (○, □, △) 0% Me_2SO; (●, ■, ▲) 20% Me_2SO.

examination of SR vesicles in the presence of Me_2SO must therefore be restricted to solvent concentrations lower than or equal to about 20% v/v, as also found by Dupont et al. (1982).

The experiments illustrated in Figure 1 were repeated for various Me_2SO concentrations, and Figure 2 shows the fluorescence changes associated, for these concentrations, with either with the *E → *E-P transition (circles) or with the *E → $E(Ca)_2$ transition (squares); Mg^{2+} was kept constant and P_i varied in Figure 2A, and P_i was kept constant and Mg^{2+} varied in Figure 2B. Figure 2 shows that (i) the apparent ATPase affinities for both Mg^{2+} and P_i increase with the concentration of Me_2SO (ii) the Ca^{2+}-induced fluorescence change (squares) is also altered by Me_2SO, (iii) with or without Me_2SO the fluorescence level obtained for full phosphorylation is significantly different from the fluorescence level of the $E(Ca)_2$ enzyme. The latter observation is slightly at variance with the results of a recent work by Dupont et al. (1982), who, however, measured fluorescence emission at a different wavelength.

Two additional results noted in the absence of Me_2SO (Figure 2B) are worth mentioning: (i) a very high Mg^{2+} concentration inhibits *E-P formation, judging by both the present data obtained from fluorescence measurements (○)

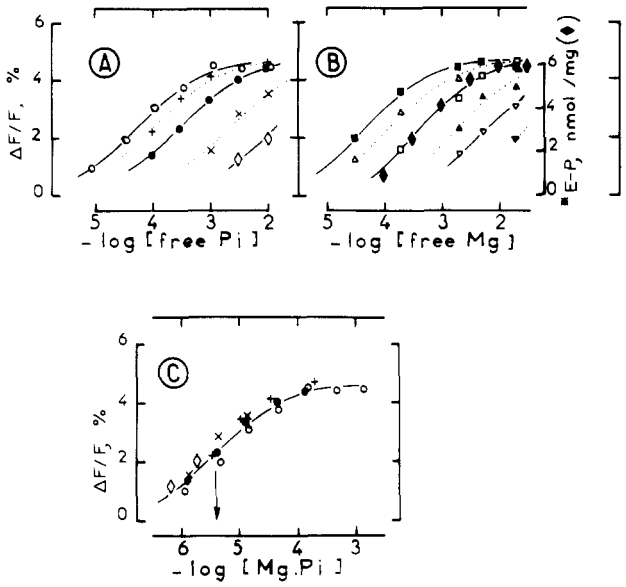

FIGURE 3: Magnesium and phosphate dependence of the *E-P level, at a fixed Me_2SO concentration (15% v/v). The *E-P level was evaluated either from fluorescence data (experimental conditions as in Figure 2) or from ^{32}P experiments (closed diamond shape, in part B): (A and C) free Mg^{2+} (mM) was 20 (○), 5 (+), 2 (●), 0.2 (×), and 0.03 (◇); (B) free P_2 (mM) was 10 (■), 3.3 (△), 1 (□, ◆), 0.33 (▲), 0.1 (▽), and 0.03 (▼).

and the chemical determinations of Martin & Tanford (1981); (ii) although in the absence of P_i the fluorescence enhancement (△) induced by addition of Mg^{2+} to the Ca^{2+}-deprived enzyme was much smaller at pH 6 that at pH 7 (Guillain et al., 1982), it was in fact also detectable at pH 6, but with reduced affinity.

In another experiment, Me_2SO was kept constant (15% v/v), and the *E-P-related fluorescence enhancement was measured for various free Mg^{2+} and P_i concentrations and plotted either as a function of P_i for various Mg^{2+} concentrations (Figure 3A) or as a function of Mg^{2+} for various P_i concentrations (Figure 3B). We also performed a series of chemical determinations of phosphoenzyme with [^{32}P]phosphate, for which the results (also plotted in Figure 3B) were not distinguishable from the fluorescence results [compare open squares (fluorescence data) and closed diamonds shapes (^{32}P data)].

Note that (i) the maximum *E-P level is high, implying full phosphorylation (about 6 nmol/mg, see right ordinate scale in Figure 3B), (ii) the maximum *E-P level can apparently be reached for infinite free P_i concentrations, even at low concentrations of Mg^{2+} in the free form (see Discussion), and (iii) changing the concentration of an ion by 1 order of magnitude shifts the affinity for the other by one order.

Selection of an adequate scheme to explain *E-P formation requires the Mg·P_i complex to be considered as a possible ligand (Kolassa et al., 1979). When our data were plotted as a function of the Mg·P_i concentration, they in fact fell on the same curve, whose affinity was about 4–5 μM (Figure 3C). This is at variance with the equilibrium *E-P levels measured in the absence of Me_2SO, which do *not* fall on the same curve when they are plotted as a function of Mg·P_i.

Phosphorylation Kinetics in the Presence of Me_2SO at pH 6. In a previous report, we suggested that monitoring the *E-P-related fluorescence signal allowed measurement of the overall time course of enzyme phosphorylation or dephosphorylation (Lacapère et al., 1981), and later ^{32}P experiments confirmed the fluorescence data (Inesi et al., 1982, 1983). We have now definitely established that *E-P formation is parallel to fluorescence enhancement, both in the presence of Me_2SO (see Figure 5) and in its absence (Guillain et al., 1984).

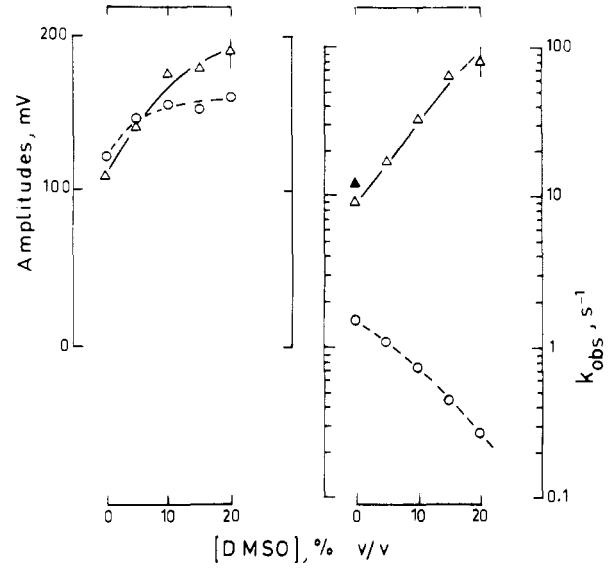

FIGURE 4: (Right) Effect of Me_2SO on the rate constant of ATPase dephosphorylation (circles) or phosphorylation (triangles). (Phosphorylation) Ca^{2+}-deprived SR, preincubated with 20 mM total Mg^{2+}, was mixed with a buffer containing 20 mM total P_i (final concentration 10 mM) and 20 mM Mg^{2+}. (Dephosphorylation) The enzyme syringe contained 2 mM EGTA, 10 mM P_i, and a variable amount of Mg^{2+} (as in Figure 3). Enzyme was dephosphorylated by mixing it with a solution containing 2 mM EGTA, 10 mM P_i, and 20 mM EDTA. Stopped-flow fluorescence was observed with a cutoff MTO 324 filter, and the rate constant of the monoexponential rise (or drop) was plotted. The closed triangle value is taken from Lacapère et al. (1981). (Left) Amplitude of the fluorescence change (initial fluorescence level was 5 V). All media contained 120–150 mM Mes–Tris (pH 6, 20 °C) and 2 mM EGTA.

The results shown in Figure 4 were obtained from stopped-flow fluorescence. The right panel (circles) shows that Me_2SO slowed down the rate of EDTA-induced ATPase dephosphorylation, in agreement with previous observations by de Meis et al. (1980); a similar conclusion had in fact also been drawn earlier by The & Hasselbach (1977) and Shigekawa & Akowitz (1979) using ATP-derived phosphoenzyme. In contrast, 0–20% Me_2SO stimulated the rate of enzyme phosphorylation, measured at high Mg^{2+} and P_i concentrations (Figure 4, right panel, triangles), a conclusion different from the one obtained previously in the presence of 40% Me_2SO and a low P_i concentration (de Meis et al., 1980; see Figure 6).

We measured the kinetics of *E-P formation or hydrolysis in parallel fluorescence and ^{32}P experiments. Some of the results are indicated in Figure 5. The left panel shows EDTA-induced dephosphorylation at 15% Me_2SO, which was very slow; the right panel shows the very fast rate of fluorescence enhancement observed at 15% Me_2SO, in the presence of high Mg^{2+} and P_i concentrations (as described in Figure 4 above). With these concentrations, the first point we were able to obtain with our multimixing device, at about 25 ms, was already close to the final level, confirming the very high rate of ATPase phosphorylation and the parallel between the rise in fluorescence and the formation of *E-P (additional data are given in Figure 6D).

Figure 6 shows how, when Me_2SO was kept constant at 15% v/v, the kinetics of the phosphorylation reaction were affected by varying the free P_i, in the presence of either 20 (triangles) or 2 mM (circles) free magnesium. Phosphorylation was monitored by stopped-flow fluorescence in Figure 6A,B, and chemical quenching measurements were included in Figure 6D. Figure 6B shows that rate constants were increasing functions of the P_i concentration, as we established earlier

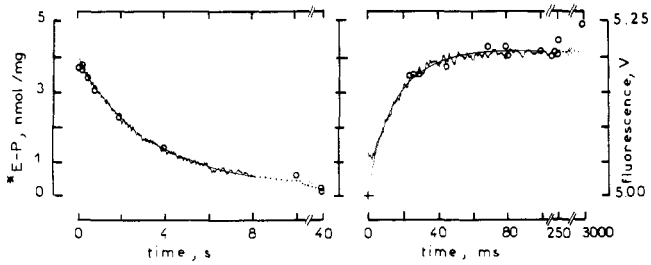

FIGURE 5: Comparison of measurements of enzyme dephosphorylation (left) or phosphorylation (right) at 15% Me_2SO, either by stopped-flow fluorescence [(continuous curve) fluorescence was detected through a B330 interference filter] or by chemical quenching procedures with [^{32}P]phosphate and a multimixing apparatus (open circles). Conditions were similar to those of Figure 4. (Phosphorylation) Enzyme syringe contained 10 mM EGTA, 22 mM Mg^{2+}, 163 mM Mes (pH 6), 15% Me_2SO, and SR ATPase (5.3 mg/mL for the ^{32}P experiments); substrate syringe contained 10 mM EGTA, 22 mM Mg^{2+}, 20 mM P_i, 130 mM Mes, and 15% Me_2SO. (Dephosphorylation) Enzyme syringe contained 5 mM EGTA, 10 mM P_i, 0.24 mM Mg^{2+}, 130 mM Mes (pH 6), 15% Me_2SO, and ATPase (5 mg/mL for the ^{32}P experiments); the substrate syringe contained 5 mM EGTA, 20 mM EDTA, 130 mM Mes, and 15% Me_2SO.

[Lacapère et al., 1981; see also Rauch et al. (1977) and Inesi et al. (1982, 1983)]. Figure 6B also shows that there is roughly a factor of 10 between the rate constants obtained at 2 and 20 mM free magnesium, respectively.

When the phosphorylation rate constants were plotted as a function of the Mg·P_i complex concentration, they again fell on a single curve, which, when extrapolated to zero Mg·P_i (see arrow in Figure 6D), gave the dephosphorylation rate actually measured. This is shown in Figure 6D, where rate constants, which spread over 3 orders of magnitude, are plotted for convenience on a log scale. All our fluorescence data, as well as the chemical quenching ^{32}P determinations (open hexagonal symbols), fit on the same curve.

Note that when we tried to induce phosphorylation under two different conditions (see arrows in Figure 6B), either by adding P_i to Mg^{2+}-preincubated SR or by adding Mg^{2+} to P_i-preincubated SR, we found the same rate constant, irrespective of the order of addition of the ligands. This strengthens the possibility that the Mg·P_i concentration is the only parameter affecting the rate constant of the phosphorylation reaction.

Figure 6A,C simply shows the amplitudes of the transient fluorescence signals, which of course depend on the P_i or Mg·P_i concentration to the same degree as the *E-P levels measured at equilibrium (Figure 3). The same affinity for Mg·P_i, namely, about 4–5 μM, is derived from Figures 6C and 3C.

Oxygen Exchange Experiments at pH 6. The remarkable relevance of medium $P_i \rightleftharpoons$ HOH oxygen exchange experiments to studies of the mechanism of ATPase phosphorylation, as depicted in Scheme IV, has already been shown (Boyer et al., 1977; Hackney et al., 1980; McIntosh & Boyer, 1983; Guillain et al., 1982, 1984). Starting with highly enriched [^{18}O]P_i labeled on all four oxygen atoms ($P^{18}O_4$), reversal of enzyme phosphorylation and P_i release gives rise to the incorporation of ^{16}O atoms from water into the phosphate pool and to the appearance of P_i species labeled with either three, two, one, or zero ^{18}O oxygen atoms (i.e., $P^{18}O_3$, $P^{18}O_2$, $P^{18}O_1$, $P^{18}O_0$, Figure 7A,B).

Scheme IV

$$*E + S \underset{k_{-1}}{\overset{k_1}{\rightleftharpoons}} *E{\cdot}S \underset{k_{-2}}{\overset{k_2}{\rightleftharpoons}} *E\text{-}P + H_2O$$

A useful parameter that can be obtained from such measurements is the probability P_c that a bound P_i molecule will

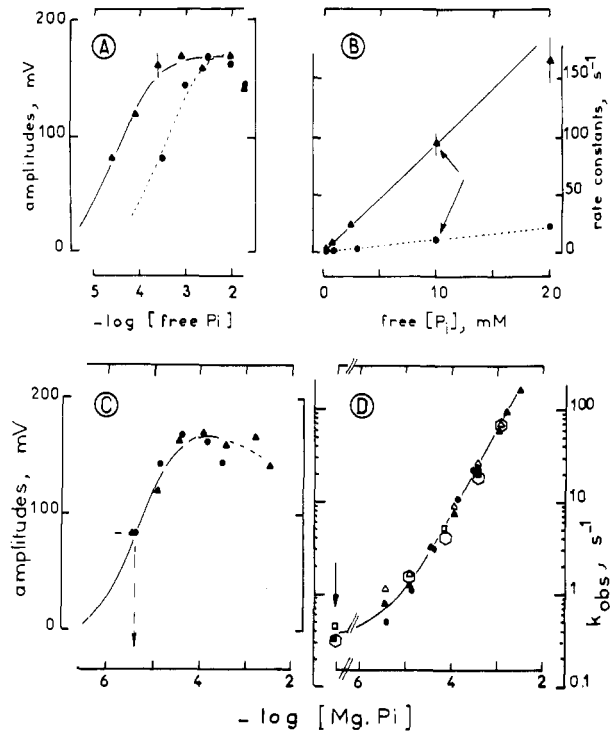

FIGURE 6: Kinetics of the phosphorylation reaction in the presence of 15% Me_2SO. (A and B) Amplitudes and rate constants observed in stopped-flow fluorescence experiments with an interference B 330 filter, with either 20 (▲) or 2 mM (●) free magnesium; (C and D) amplitudes and rate constants, plotted as a function of [Mg·P_i]. Panel D includes additional data, namely, the fluorescence measurements obtained with a cutoff MTO 324 filter, as in Figure 4 (open symbols), and chemical determinations of the rate constant, as in Figure 5 (open hexagons). The significance of the arrows in panels B and D is given in the text.

undergo the covalent reaction rather than be released into the medium: $P_c = k_2/(k_2 + k_{-1})$. Hackney & Boyer (1978) have shown that P_c can be deduced simply by comparing the loss of the $P^{18}O_4$ species (k_4) with the average loss of total ^{18}O in the four oxygen-containing P_i (k_{av}). This result can be qualitatively explained as follows: if many exchanges occur each time a $P^{18}O_4$ molecule binds to the enzyme, i.e., if P_c is close to 1, the released phosphate molecule will carry a number of ^{16}O atoms statistically close to 4, and the average enrichment in ^{18}O of the P_i pool will drop concomitantly with the residual amount of $P^{18}O_4$ molecules ($k_{av} \simeq k_4$). On the other hand, if P_c is close to zero, there is only a small probability that the $P^{18}O_4$ molecules bound to the enzyme will be exchanged, and the few $P^{18}O_3$ molecules formed via enzyme phosphorylation and dephosphorylation will almost certainly be released into the medium rather than undergo a second exchange cycle: therefore, the average enrichment in ^{18}O of the total P_i pool will drop 4 times more slowly than the residual amount of $P^{18}O_4$ molecules ($k_{av} \simeq k_4/4$). If P_c lies between 0 and 1, the ratio k_4/k_{av} will be between 4 and 1 (for the precise equation, see Experimental Procedures).

If the phosphoenzyme level (*E-P) is known, another critical parameter that can be obtained from oxygen experiments is the true rate of *E-P hydrolysis. This rate, k_{-2} (Scheme IV), can be calculated from the relation

$$v_{ex,obsd} = k_{-2}[*E\text{-}P]\alpha$$

This relation simply means that the measured $v_{ex,obsd}$, i.e., the observed flux of ^{18}O atoms between P_i and water deduced from the rate of loss of average P_i enrichment [V in Hackney et al. (1980)], is not exactly equal to k_{-2}[*E-P], the true total flux

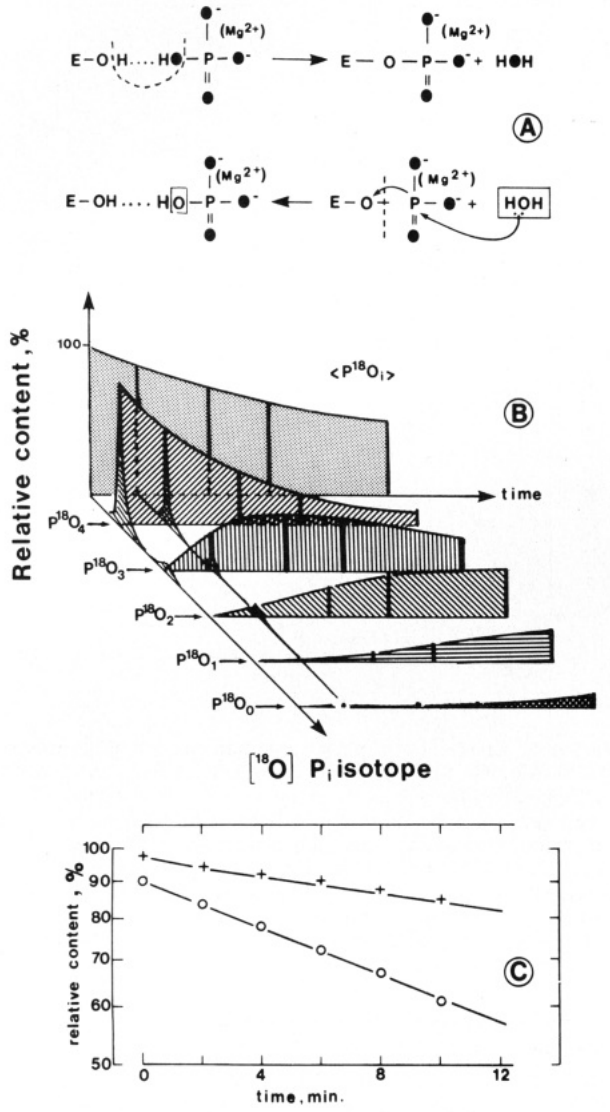

FIGURE 7: (A) Exchange cycle. (● and O) ^{18}O and ^{16}O atoms. (B) Time dependence of the various isotopic species of the phosphate pool, in a typical oxygen exchange experiment [data taken from Table II—no calcium–in Ariki & Boyer (1980)]. (C) Time dependence of the relative amount of the $P^{18}O_4$ species (O), compared to the average ^{18}O content of all phosphate species (+), in our ^{18}O exchange experiment: 6.25 mM highly ^{18}O enriched phosphate was added to a medium containing 1 mg/mL SR protein in 130 mM Mes–Tris, 15% Me_2SO, 2 mM EGTA, and 21.25 mM total Mg (pH 6, 20 °C; final free $[Mg^{2+}] \simeq 20.5$ mM, $[Mg{\cdot}P_i] \simeq 0.8$ mM).

of species across step 2 [ρ in Hackney et al. (1980)]. α is a correcting factor, close to 1 for small P_c but equal to 0 for $P_c = 1$, meaning that, when step 2 is reversed several times before P_i release, some reversals do not result in further loss of the ^{18}O content of medium P_i; α is the fraction of reversals that leads to loss of ^{18}O and can be calculated from P_c (for the precise equation, see Experimental Procedures).

In our experiments, we measured oxygen exchange under the following conditions: 15% Me_2SO, 1 mg/mL protein, 6.25 mM P_i, 21.25 mM Mg^{2+}, pH 6, and 20 °C. We found $k_4/k_{av} \simeq 2.6$, and therefore, $P_c = 0.45 \pm 0.08$ and $\alpha = 0.83$; $t_{1/2}$ for the loss in average ^{18}O enrichment was about 50 min, and therefore, $v_{ex,obsd} \simeq 345$ nmol/(mg min) and $v_{ex,obsd}/\alpha \simeq 415$ nmol/(mg min) = 6.9 nmol/(mg s). Since under these conditions the *E-P level was about 6 nmol/mg (Figure 3), we obtained $k_{-2} \simeq 1\ s^{-1}$. Even if we allow for up to 20% experimental errors during temperature equilibration, protein concentration calibration, etc., this value is significantly higher than the dephosphorylation rate constant measured (Figure 6D) from fluorescence or chemical quenching determinations.

This difference between the two sets of data is completely consistent with the partition coefficient P_c being significantly different from 0. Whenever P_c is larger than 0, the rate observed for enzyme dephosphorylation and P_i release into the medium in a dephosphorylation experiment is *not* equal to the true k_{-2} hydrolysis rate; the observed dephosphorylation rate, k_{OFF}, is equal to $k_{-2}(1 - P_c)$ (see Experimental Procedures), i.e., about $k_{-2}/2$ under our conditions in the presence of Me_2SO.

Perturbation by Me_2SO or Glycerol of ATPase Interaction with Mg^{2+} at pH 7: Fluorescence Data. The results shown in Figure 1 gave the first indication that Me_2SO reduced the magnesium-induced intrinsic fluorescence enhancement observed with Ca^{2+}-deprived SR vesicles. We previously investigated in some detail this effect of magnesium in the absence of solvent (Guillain et al., 1982). Since the experiments illustrated in Figure 1 had been performed at pH 6, i.e., under conditions unfavorable for detection of this type of ATPase-magnesium interaction, they were repeated at neutral pH. The upper trace in Figure 8A shows the already documented Mg^{2+}-induced spectral shift in the absence of solvent, which resulted in Mg^{2+}-induced fluorescence enhancement at the chosen emission wavelength of 320 nm. Further addition of P_i under these conditions (pH 7) only allowed formation of a small amount of phosphoenzyme, and fluorescence was only slightly further enhanced. The lower trace demonstrates that the Mg^{2+}-induced fluorescence enhancement was greatly reduced in the presence of Me_2SO, whereas phosphoenzyme formation was, as expected, greatly stimulated. Note that this Me_2SO-induced stimulation of the *E-P-related fluorescence enhancement was also observed (not shown) when a cutoff filter was used to detect fluorescence, i.e., in the absence of any magnesium-related signal.

Figure 8B quantifies the above observation: under our conditions, i.e., at pH 7, 20 °C, and absence of potassium, the fluorescence change induced by adding Mg^{2+} to calcium-deprived SR vesicles (open circles) was virtually abolished in the presence of increasing amounts of Me_2SO, whereas the change observed upon further calcium addition to the Mg^{2+}-saturated SR (closed circles) was maintained in the presence of Me_2SO.

We repeated similar experiments in the presence of glycerol. There were two reasons for studying SR perturbation by glycerol: first, glycerol has been shown to resemble Me_2SO in its ability to abolish or reduce the pH and temperature dependence of ATPase phosphorylation by P_i (de Meis et al., 1980); second, glycerol was used as an antifreeze solvent in a recent study by Dupont (1982). To keep close to the conditions of the latter work, we tested the effect of glycerol in the presence of 100 mM KCl and 5 mM Mg^{2+} (pH 7). It turned out to be very similar to that of Me_2SO; namely, the fluorescence change observed on addition of magnesium to Ca^{2+}-deprived SR was virtually abolished in the presence of increasing amounts of glycerol (Figure 8C).

Following up our previous observations (Champeil et al., 1983), we then investigated, in the presence of solvent, the kinetics of the fluorescence rise after addition of a high calcium concentration to Ca^{2+}-deprived SR preincubated with magnesium (Figure 9). In contrast with the biphasic pattern observed in the absence of organic solvent, we found that the amplitude of the fast phase (closed symbols) dropped to nearly zero for a Me_2SO concentration of about 20% v/v (Figure 9A) or for a glycerol concentration higher than 30% (Figure 9C). In addition, Me_2SO and glycerol drastically slowed down the

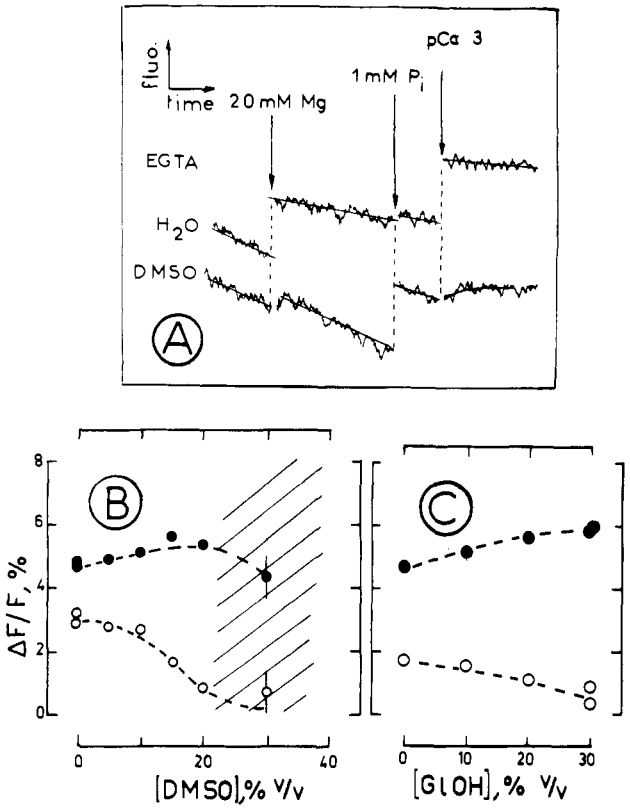

FIGURE 8: Me_2SO and glycerol dependence of the intrinsic fluorescence changes induced by addition of ligands to calcium-deprived SR vesicles. The fluorometer cuvette contained 100–150 mM Mops (pH 7, 20 °C), 2 mM EGTA, and 40–50 μg of SR protein/mL. Excitation wavelength was 290 nm. (A) Emission wavelength was 320 nm. Magnesium, P_i, and calcium were added in that order. The Me_2SO concentration was 0 (upper curve) or 20% v/v (lower curve). (B) Emission wavelength was 330 nm. For various Me_2SO concentrations, 20 mM Mg^{2+} was first added and the fluorescence enhancement measured (○); 3 mM total calcium (final pCa 3) was added subsequently, and the new fluorescence change was measured (●). Solvent concentrations higher than 20% were avoided because of vesicle aggregation. When the MTO cutoff filter was used to detect emitted fluorescence (not shown), the Mg^{2+}-induced fluorescence change was hardly detectable (Guillain et al., 1982), and the magnitude of the Ca^{2+}-induced fluorescence change was slightly reduced by Me_2SO [cf. (Σ) in Figure 9A]. (C) Glycerol was used instead of Me_2SO. The medium contained 0–30% v/v glycerol, 100 mM KCl, 50 mM Mops–Tris (pH 7, 20 °C), 40–50 μg/mL SR protein, and 2 mM EGTA; 5 mM Mg was added, and the fluorescence change was measured (○); 3 mM Ca was added subsequently (final pCa 3), and the new fluorescence change was measured (●). Emitted light was detected as in (B).

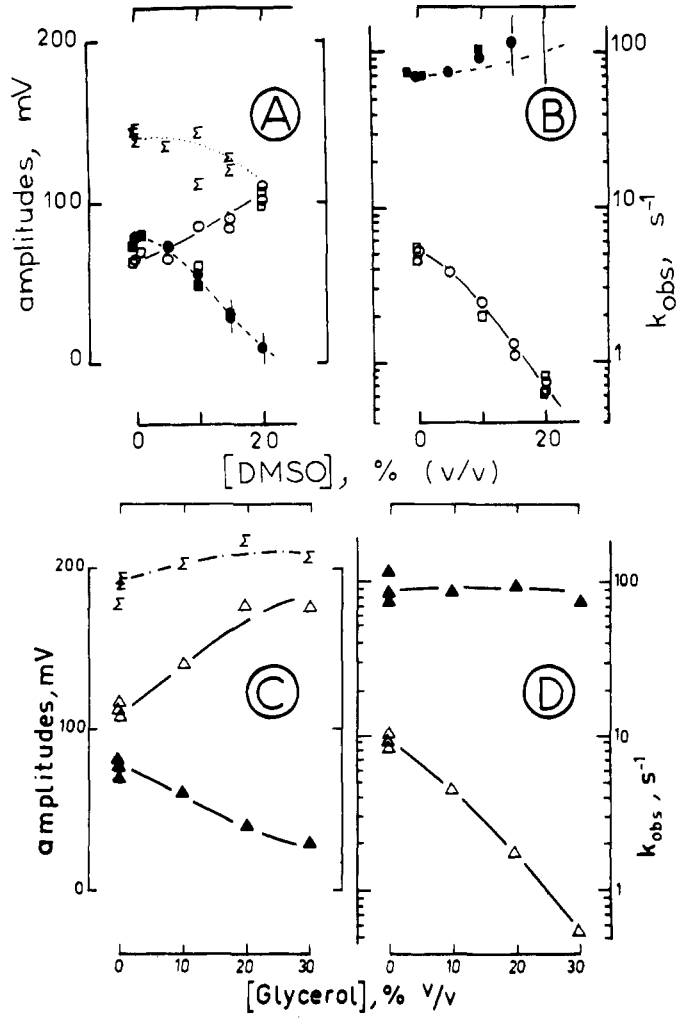

FIGURE 9: Me_2SO (A and B) and glycerol (C and D) dependence of the kinetics of the fluorescence changes induced by calcium in the presence of magnesium. Amplitudes (left) and rate constants (right) of the slow (open symbols) and fast (closed symbols) phases of the fluorescence rise. Enzyme syringe contained SR and 2 mM EGTA; substrate syringe contained 4 mM Ca^{2+} (i.e., pCa 3 after mixing). (Σ) Total Ca^{2+}-induced fluorescence change (fast + slow amplitude). Excitation wavelength was 290 nm. (A and B) Medium contained 150 mM Mops (pH 7), 20 mM Mg^{2+}, and Me_2SO; emitted light was analyzed with the MTO 324 cutoff filter. (C and D) Medium contained 50 mM Mops, 100 mM KCl, 5 mM Mg^{2+}, and glycerol; emitted light was analyzed with a Balzer B 330 filter.

rate constant of the slow phase (open symbols in Figure 9B,D).

In the absence of Me_2SO, the interaction of Mg^{2+} with the Ca^{2+}-deprived SR is also reflected by a specific kinetic pattern of the fluorescence response to the addition of various concentrations of calcium in the presence of magnesium [Figure 6 in Champeil et al. (1983)]. Figure 10 shows how this typical pattern disappeared in the presence of increasing Me_2SO concentrations. For moderate Me_2SO concentrations (10%, Figure 10A,B) and high calcium concentrations, the pCa dependence of the observed fluorescence rise still revealed that a fast phase (closed symbols) made a small contribution to the total fluorescence change; the amplitude of this fast phase rose for the same range of calcium concentrations as the rate constant of the slow phase. In the presence of 20% Me_2SO, however (Figure 10C,D), the fast phase was absent, irrespective of the calcium concentration, and significantly, in this case, the rate constant of the slow phase did *not* rise with the calcium concentration; this observation is consistent with our previous explanation that in the absence of solvent this rise in the slow rate constant was the result of the appearance of readily available calcium binding sites after preincubation with magnesium.

Comparison of Figure 10A,C with Figure 6 in Champeil et al. (1983) suggests that in the presence of Me_2SO and 20 mM Mg^{2+} the enzyme had a slightly higher affinity for calcium than in the absence of the solvent. This was confirmed in simple equilibrium titrations of the ATPase fluorescence response to calcium in the presence of 20 mM Mg^{2+}; they showed that $pCa_{1/2}$ was about 5.8 in the presence of 20% Me_2SO compared to 5.6 in the absence of Me_2SO (not shown). Note that we verified that the Ca·EGTA dissociation constant was not affected by 20% v/v Me_2SO (see Experimental Procedures).

From Figures 8–10 it is clear that in the presence of Me_2SO or glycerol magnesium was no longer able to exert the two effects on the E_2 or *E conformation of the enzyme characterized in a previous work, i.e., it neither shifted the fluorescence of the Ca^{2+}-deprived enzyme nor allowed the appearance

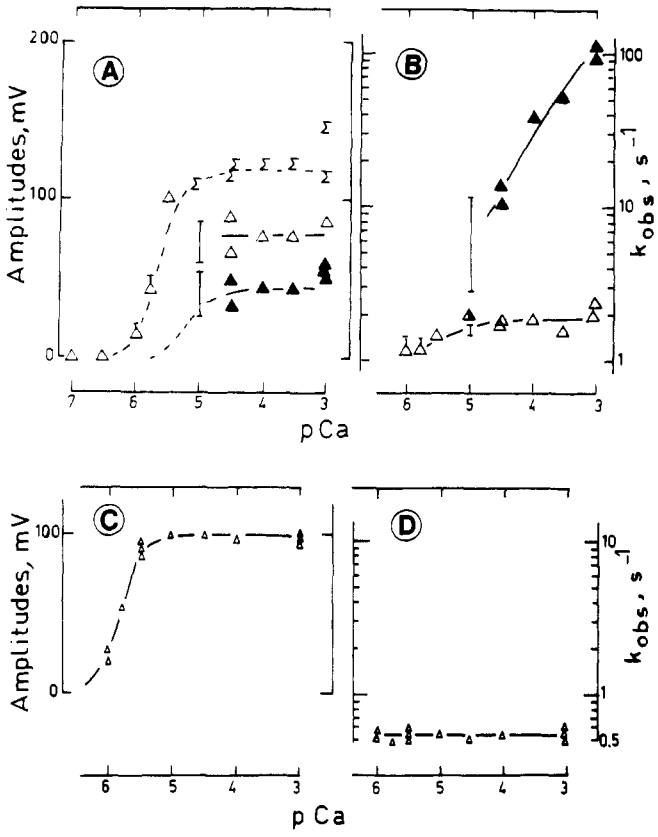

FIGURE 10: Calcium dependence of the kinetic pattern of the fluorescence changes after calcium addition in the presence of 20 mM Mg^{2+} and either 10 (A and B) or 20% (C and D) Me_2SO: amplitudes (A and C) and rate constants (B and D) of the slow (open symbols) and fast (closed symbols) phases of the fluorescence rise. In (A), (Σ total fluorescence change (slow + fast amplitudes). In (B), the fluorescence rise for pCa 5 was also analyzed as a single exponential (right solid triangle). Emitted light was analyzed through the MTO 324 cutoff filter.

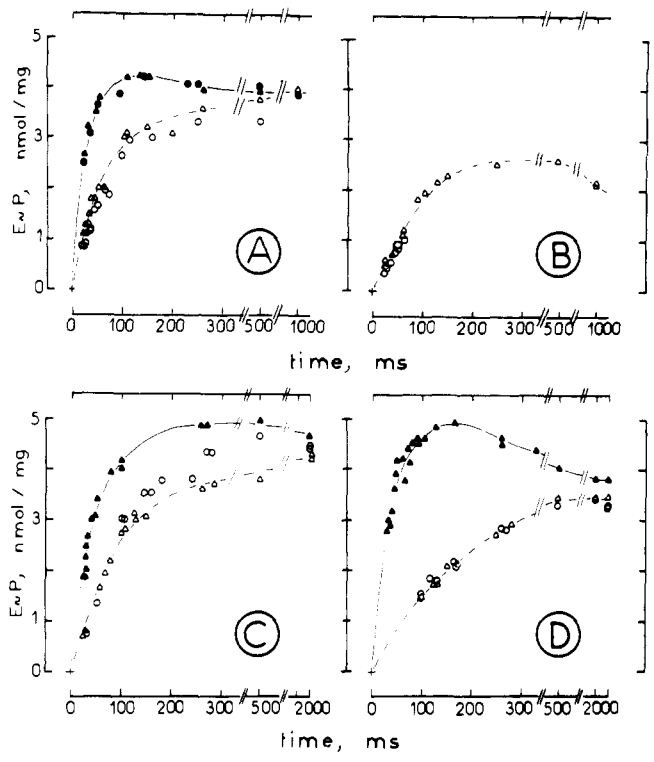

FIGURE 11: Time course of ATPase phosphorylation from [^{32}P]ATP, with or without preincubation with Ca^{2+}, EGTA, or Mg^{2+}. The final medium contained 0.18 mg/mL ATPase, 0.25 mM EGTA, 0.35 mM Ca^{2+}, and (A) 150 mM Mops (pH 7), 20 mM Mg^{2+}, and 5 μM ATP, (B) 150 mM Mops (pH 7), 20 mM Mg^{23}, and 2 μM ATP, (C) 120 mM Mops (pH 7), 20 mM Mg^{2+}, 5 μM ATP, and 20% Me_2SO, and (D) 150 mM Mes (pH 6), 20 mM Mg^{2+}, and 5 μM ATP. Symbols are as follows: (●) SR and Ca^{2+} mixed with ATP and Mg^{2+}; (▲) SR, Ca^{2+}, and Mg^{2+} mixed with ATP; (○) SR and EGTA mixed with Ca^{2+}, Mg^{2+}, and ATP; (△) SR, EGTA, and Mg^{2+} mixed with Ca^{2+} and ATP.

of a form of ATPase capable of fast calcium binding. These effects of Mg^{2+} had been tentatively attributed to competition between Mg^{2+} and Ca^{2+} for a common site, and the Me_2SO-induced slight shift in $pCa_{1/2}$ noted above is in agreement with the conclusion that Me_2SO counteracted the magnesium competition with calcium [note, however, that even in 20% Me_2SO, pH 7, magnesium still shifted the pCa dependence of the SR fluorescence ($pCa_{1/2} \simeq 5.8$ for 20 mM Mg^{2+} compared to $pCa_{1/2} \simeq 6.4$ for zero Mg^{2+}; data not shown)].

Interaction of SR ATPase with Mg^{2+}, As Revealed by Kinetics of Phosphorylation from ATP. It well-known that the Ca^{2+}-deprived conformation of SR ATPase cannot be phosphorylated by ATP; when ATP and Ca^{2+} are added to Ca^{2+}-deprived ATPase, phosphorylation is delayed due to the Ca^{2+}-induced *E → E transition. In our previous work, we had suspected that at pH 7, preincubation with magnesium of the Ca^{2+}-deprived ATPase would modify this phosphorylation time course. We therefore repeated these experiments with and without Me_2SO (Figure 11). However, we could not completely confirm the previous observations. Instead, we found that preincubation with magnesium of the Ca^{2+}-deprived ATPase only had a slight effect on the phosphorylation time course observed after simultaneous addition of Ca^{2+} and either 5 (Figure 11A) or 2 μM (Figure 11B) ATP (open triangles vs. circles in this figure). Both with and without preincubation with Mg^{2+}, the rate of phosphorylation was faster than the rate of the Ca^{2+}-induced transition in the absence of ATP (3–4 s^{-1}): thus, we found about 10 s^{-1} for 2 μM ATP and about 15 s^{-1} for 5 μM ATP. As expected, phosphorylation after addition of ATP to Ca^{2+}-saturated enzyme was fast (closed symbols in Figure 11A).

At pH 6 (Figure 11D), preincubation with Mg^{2+} did not modify the time course of phosphorylation after addition of ATP and Ca^{2+} (5–6 s^{-1} for 5 μM ATP, open symbols), and again, as in previous measurements (Guillain et al., 1981), this rate was faster than the rate of the *E → E transition in the absence of nucleotide (1.5 s^{-1}).

In contradiction therefore with our previous suggestion, Figure 11A,D shows that acceleration by ATP of protein isomerization does not require ATPase preincubation with magnesium. This is now fully consistent with the original work of Scofano et al. (1979). One of the significant experimental differences between the present results and our previous data [Figure 7 in Champeil et al. (1983)] is probably that in the present work enzyme was diluted in the EGTA-containing medium immediately before phosphorylation. Therefore, what now appears to be correlated with the pH-dependent effect of Mg^{2+} is a protective effect against partial denaturation, i.e., an effect protecting the capacity of ATP to accelerate isomerization.

Figure 11C shows a repetition of the pH 7 experiment in the presence of Me_2SO. Starting from Ca^{2+}-deprived ATPase (open symbols), phosphorylation was slowed down compared to the situation prevailing in the absence of Me_2SO (cf. Figure 11A), confirming that the Ca^{2+}-induced isomerization is slowed down by Me_2SO, although still accelerated by ATP (compare with Figure 9B).

Interaction of SR ATPase with Mg^{2+}, As Shown by Kinetics of Phosphorylation from P_i at pH 7. It is well-known that

Table I: Almost Complete Phosphorylation of SR ATPase by P_i at pH 6[a]

[free P_i] (mM)	[Me_2SO] (v/v)	[*E-P] (nmol/mg)
10	0	5.3–5.7
10	15	6.3
10	30	6.3
1	0	1.5
1	15	6

[a] Phosphoenzyme formation from P_i was measured with [^{32}P]P_i, essentially as in Lacapère et al. (1981). The medium contained 110–150 mM Mes–Tris, no potassium, 8 mg of SR protein/mL, 20 mM EGTA, 0–30% Me_2SO, and either 22.5 mM Mg^{2+} + 12.5 mM P_i or 20 mM Mg^{2+} + 1.25 mM P_i. The protein-loaded filter was extensively washed to reduce nonspecific background radioactivity.

when Ca^{2+}-deprived ATPase is supplemented with magnesium and phosphate, measured phosphoenzyme levels are maximal at a rather acidic pH (pH 6) and that this pH dependence vanishes in the presence of Me_2SO [see de Meis et al. (1980)]. Here, we wish to demonstrate that this behavior reflects the pH-dependent Me_2SO-sensitive effect of Mg^{2+} on the Ca^{2+}-deprived ATPase.

(i) Phosphorylation May Be Almost Complete at pH 6. At pH 6 and in the absence of potassium, covalent bond formation is a thermodynamically favorable process ($k_{phosph}/k_{hyd} \gg 1$, in Schemes I and II); this has now been unambiguously demonstrated (Lacapère et al., 1981; Inesi et al., 1984; Guillain et al., 1984). Therefore the maximal amount of phosphoenzyme formed at pH 6 should be close to the total number of active polypeptide chains, even in the absence of Me_2SO. Table I shows that this was definitely the case, since the total number of sites in our SR preparation can be estimated at 6.5 nmol/mg of protein, if one considers that 75% of the protein consists of the M_r 115 000 ATPase [compare also with the phosphoenzyme levels we were able to measure (Figure 11) after Ca^{2+}-dependent phosphorylation from ATP]. To obtain these high *E-P levels, we used very high concentrations of Mg^{2+} and P_i (20 and 10 mM free concentrations, respectively). At these nearly saturating concentrations, addition of Me_2SO only slightly enhanced the *E-P level, in contrast with the greater effect of Me_2SO observed for a lower P_i concentration. Note that this experiment was performed at pH 6, so that the inhibitory effect of 20 mM Mg^{2+} was very small. Previous unsuccessful attempts (including our own) to obtain full phosphorylation at pH 6 might have been due to the use of unduly low ligand concentrations and/or partly inactivated preparations.

(ii) Preincubation with Magnesium at pH 7 Depletes the Phosphate-Reactive Conformation, Resulting in Less Than Stoichiometric Phosphorylation. It is no simple matter to design an experiment demonstrating that Mg^{2+} is either "on" the pathway toward phosphorylation (Schemes I or II) or "off" this pathway (Scheme III). Such a crucial experiment is depicted in Figures 12 and 13. It relies heavily on our previous finding that addition of magnesium to calcium-deprived enzyme only depletes the *E conformation slowly, the rate constant of this *E → E$^?$Mg transition being 3–4 s^{-1} (Guillain et al., 1982). In contrast, we expected phosphorylation to be fast for high levels of Mg^{2+} and P_i. This would have implied that addition of large amounts of magnesium to ATPase preincubated with P_i would allow fast phosphorylation of the reactive *E conformation (*E → *E-P, see Scheme III) and that the inhibitory effect of Mg^{2+} (*E → E$^?$Mg) would only occur slowly, possible giving rise to a slight overshoot. For ATPase molecules preincubated with magnesium, the implication would be, on the contrary, that, since only a fraction of these molecules would exhibit the substrate-reactive *E

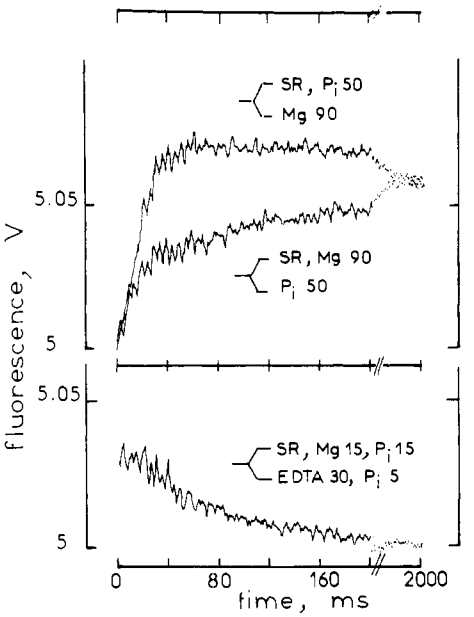

FIGURE 12: Stopped-flow fluorescence recordings during *E-P formation (upper panel) or *E-P hydrolysis (lower panel) at pH 7 in the absence of potassium. The order of ligand addition is indicated. The fluorescence signal was measured with a MTO 324 cutoff filter, thus avoiding interference from magnesium. (Upper panel) Final medium contained 100 mM Mops, 2 mM EGTA, 45 mM Mg, and 25 mM P_i; since, at pH 7, $[Mg^{2+}][P_i]/[Mg{\cdot}P_i]$ = 20 mM, free concentrations were 30 mM Mg^{2+} and 10 mM P_i. (Lower panel) Phosphorylated ATPase was dephosphorylated by adding excess EDTA. The medium contained 100 mM Mops and 2 mM EGTA. In all cases pH was 6.95 ± 0.05 after mixing. The fluorescence drift was subtracted from all curves to allow easier comparison with Figure 13.

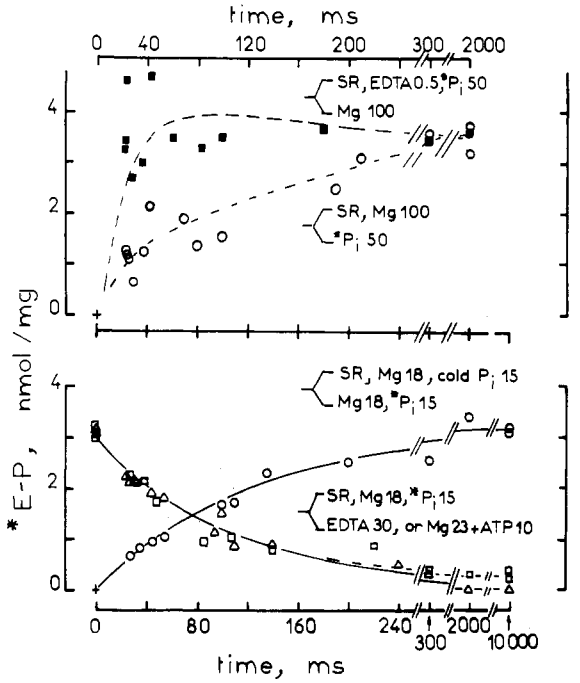

FIGURE 13: Same experiment as in Figure 12 except that *E-P was chemically determined from [^{32}P]P_i. The medium was basically the same, except that the protein concentration was much higher (4–5 mg/mL after mixing), and therefore, the EGTA concentration was raised to 10 mM; this slightly influenced the added total concentrations of ligands, since at pH 7 Mg^{2+} binds to EGTA with a dissociation constant of 25 mM. The final free concentrations are therefore the same as in Figure 12. In the upper panel, phosphorylation was initiated by adding Mg^{2+} (■) or P_i (○). In the lower panel, dephosphorylation was measured after addition of excess EDTA (△) or 5 mM Mg-ATP (□) or during an exchange reaction (○).

conformation, phosphorylation would be slower and biphasic.

We first tested this reasoning by using intrinsic fluorescence to detect *E-P formation. We chose a cutoff filter so that the interaction with magnesium per se would not give rise to fluorescence enhancement, and we adjusted osmolarities so that osmotic shrinking would not perturb the fluorescence signal (Guillain et al., 1982; Champeil et al., 1983). The final conditions selected were 30 mM free Mg^{2+} and 10 mM free P_i (pH 7), i.e. 15 mM ($Mg{\cdot}P_i$). Figure 12 (upper panel) shows that the experiment did work as anticipated, i.e., with a very high rate of phosphorylation when the enzyme was not preincubated with magnesium. Compared to this phosphorylation rate, the dephosphorylation rate, as measured in the lower panel of the figure after magnesium chelation, was much slower.

The experiment was repeated with [^{32}P]P_i and a Dionex D133 multimixing apparatus, and the resulting radioactivity measurements are shown in Figure 13, upper panel. Despite the scatter of the experimental results due to the very high total P_i concentration and therefore the poor signal-to-noise ratio, the results were completely consistent with those of Figure 12, emphasizing here again the parallel between the fluorescence signal and *E-P formation. In the lower panel of Figure 13, the dephosphorylation rate was measured by three different procedures, giving consistent results: dephosphorylation was initiated either by chelation of magnesium or by displacing phosphate by excess ATP at a constant free Mg^{2+} concentration; the dephosphorylation rate was also measured in an exchange experiment (Boyer et al., 1977). Note that, in Figure 13, hydrolysis was neither stimulated by ATP nor affected by the final Mg^{2+} concentration.

From all these data, a dephosphorylation rate close to 10 $\pm$ 2 s^{-1} was obtained; the phosphorylation rate for Mg^{2+}-free enzyme was of the order of 50 s^{-1} (see Figures 12 and 13), so that the true k_{phosph}/k_{hyd} ratio, which is larger (Lacapère et al., 1981) than the observed ratio (50 s^{-1}/10 s^{-1}), is clearly much greater than 1. The reason why the *E-P level is far from stoichiometric phosphorylation is that magnesium has an inhibitory effect at pH 7.

In contrast with the situation described above, it should be recalled here that we observed identical time courses of phosphorylation at pH 6 and in the presence of Me_2SO after addition of P_i to Mg^{2+}-preincubated ATPase or after addition of Mg^{2+} to P_i-preincubated ATPase (Figure 6B, arrows).

Discussion

Phosphorylation from P_i at pH 6 in the Presence of Me_2SO. The first point worth noting is the agreement between the results for the different techniques we used to investigate the phosphorylation reaction. In particular, fluorescence and chemical quenching methods gave completely consistent data (see Figures 3B, 5, and 6D), a finding that was also true in the absence of organic solvent (Guillain et al., 1984). Needless to say, a rate constant is more easily deduced from a stopped-flow recording than from a multimixing experiment with chemical quenching. Both techniques gave a dephosphorylation rate that differed from the true hydrolysis rate derived from oxygen exchange experiments. This difference is absolutely consistent with the high P_c value recorded in the presence of Me_2SO (see Results).

The oxygen exchange experiment allowed definite assignment of rate constants to the various steps in *E-P formation (Scheme IV). The present data confirm that *E-P hydrolysis is indeed the slowest step in this process ($k_{-2} \simeq 0.8$–1 s^{-1} at 20 °C and 15% Me_2SO). The rate of substrate binding, k_1, can also be unambiguously determined by combining the available information about k_{-2} (see above), the ratio between k_2 and k_{-1} (derived from P_c), and the apparent ATPase affinity for the substrate, which is a combination of all the k_i. When $Mg{\cdot}P_i$ is taken as the substrate (Figures 3C and 6C), the bimolecular rate constant k_1 can be calculated[2] at about 2.4 $\times$ 10^5 M^{-1} s^{-1}. For 20 mM Mg^{2+} and 100 μM P_i (and therefore 14 μM $Mg{\cdot}P_i$), i.e., for a situation in which more than half of the enzyme is phosphorylated, binding consequently takes place at a pseudo molecular rate around 3 s^{-1}, i.e., much more slowly than the covalent bond formation k_2. Our data therefore show that, for moderate substrate concentrations, binding is slow compared to covalent bond formation. Up till now, we and many others had assumed the opposite.

Only a lower limit for k_2 can be obtained from our data: $k_2 \geq 250$ s^{-1}. This is because the k_{obsd} vs. [substrate] plot is almost linear (Figure 6B), so that we cannot determine precisely the maximal k_{obsd} value. Because the k_2/k_{-1} ratio is known from P_c, we can also obtain a lower limit for k_{-1}: $k_{-1} \geq 300$ s^{-1}.

Therefore, the affinity of the initial step, i.e., binding of the $Mg{\cdot}P_i$ substrate, is poorer than 1.2 mM. As regards the second step, the high k_2/k_{-2} ratio implies that acyl phosphate formation is thermodynamically favored. Knowles & Racker (1975) had pointed out some years ago that nothing was known about the free energy of hydrolysis of an acyl phosphate buried in a hydrophobic region; de Meis et al. (1980) explicitly suggested that in the absence of Ca^{2+} the catalytic site of the ATPase was hydrophobic, allowing acyl phosphate formation to be thermodynamically favored. Figure 6D confirms that the experimental data fit reasonably with the following set of constants, taking $Mg{\cdot}P_i$ as the substrate: $k_1 = 2 \times 10^5$ M^{-1} s^{-1}; $k_{-1} = 300$ s^{-1}; $k_2 = 250$ s^{-1}; $k_{-2} = 0.8$ s^{-1}. In the absence of solvent, k_{-2} is 1.5–2 s^{-1} under otherwise similar conditions; the Me_2SO-induced slowing down of the hydrolysis rate can at least partially be accounted for by the lower water activity in the Me_2SO–water mixture (Dupont & Pougeois, 1983).

The next point requiring discussion is of course our suggestion that in the presence of Me_2SO $Mg{\cdot}P_i$ is the substrate for phosphorylation. This conclusion was not reached by de Meis and co-workers, who also investigated the Mg^{2+} and P_i dependence of the *E-P level but supported the conventional random binding Scheme I (de Meis et al., 1982). In this connection, however, we would like to make the following points: (i) when we tried to fit our equilibrium data (Figure 3) to the conventional Scheme I, the best fits were found when the association constant for free P_i (K_2 in Scheme I) was taken as 0; (ii) the double-reciprocal plots, shown by Kolassa et al. to be useful representations in water, become both inconvenient and unnecessary in the presence of Me_2SO, since the range of useful substrate concentrations spreads over 3 orders of magnitude and since the maximum *E-P level can be estimated without extrapolation, due to the Me_2SO-enhanced affinity; (iii) Scheme I implies that for infinite free P_i, different *E-P levels should be obtained at low or high free Mg^{2+} concentrations, which is not the case (Figure 3A). Our claim that the maximum *E-P level can be reached at both low and high Mg^{2+} concentrations is in fact also supported by results reported by de Meis et al. in their first work dealing with Me_2SO [see Figure 4 in de Meis et al. (1980)].

[2] Since, in step 2, k_2 is much larger than k_{-2}, substrate affinity, expressed as the dissociation constant K_{diss}, is simply $k_{-1}k_{-2}/(k_1k_2)$; when $Mg{\cdot}P_i$ is taken as the substrate, $K_{diss} \simeq 5 \times 10^{-6}$ M (Figures 3C and 6C); $k_{-2} \simeq 1$ s^{-1}; since $P_c \simeq 0.45$, $k_2/k_{-1} = P_c/(1 - P_c) \simeq 0.82$; we can then calculate k_1: $k_1 \simeq 2.4 \times 10^5$ M^{-1} s^{-1}.

Scheme V

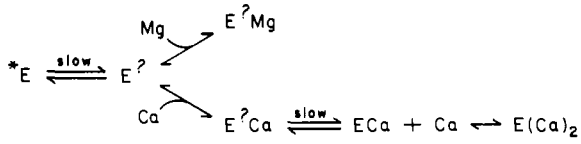

In addition, we showed that rate constants for the phosphorylation reaction depended exclusively on the $Mg{\cdot}P_i$ concentration and, in particular, not on the order in which the free ions were added (Figure 6B,D). We therefore see no reason for postulating any other mechanism but that of Scheme II, in which $Mg{\cdot}P_i$ is the actual substrate for ATPase phosphorylation in the presence of Me_2SO. Note also that the ATPase is fully reactive for phosphorylation, an earlier controversial point that now appears to have been cleared up (Barrabin et al., 1984).

Interaction of Mg^{2+} with Ca^{2+}-Deprived ATPase in the Presence or Absence of Me_2SO. We summarized in the introduction the various lines of evidence suggesting that magnesium might be able to deplete the so-called *E conformation of the SR ATPase, a conformation that is supposed to be devoid of high-affinity calcium binding sites (de Meis & Vianna, 1979). The mechanism of this effect of magnesium is not yet quite clear. Nevertheless, competition between Mg^{2+} and Ca^{2+} after a slow conformational change rendering one calcium site accessible from the outside of the vesicles was suggested (Vianna, 1975; Loomis et al., 1982; Guillain et al., 1982; Champeil et al., 1983) and might be described as in Scheme V.

We used the E?Mg notation, since it is not yet clear how closely this species resembles the conformation E (also called E_1) known to exist in the presence of calcium. We obtained data supporting essentially the same scheme, in both the absence and presence of potassium (Figures 8C and 9C). Addition of dimethyl sulfoxide or glycerol, on the other hand, severely perturbed the typical pattern observed in the absence of either of these agents; Me_2SO and glycerol also drastically slowed down individual rate constants (Figures 8–10). Such sensitivity to these agents is not in itself surprising, since water-soluble proteins like glycogen phosphorylase *b*, hemoglobin, and *Escherichia coli* aspartate transcarbamoylase, known to experience allosteric regulations, also interact with solvents (Dreyfus et al., 1978; Cordone et al., 1979; G. Hervé et al., personal communication). The effect of glycerol, however, is worth specific comment, since this agent has been used as an antifreeze: we found that 30% glycerol partially prevented the Mg^{2+}-induced appearance of a fast phase in the fluorescence rise. On the other hand, Dupont reported that one calcium binding site was available at the outer surface of the vesicles in the presence of KCl, magnesium, and 30% glycerol at −10 °C (Dupont, 1982): in the latter experiments, temperature might therefore be a significant parameter worth reinvestigation.

Implications for Mechanism of Phosphorylation from P_i in the Absence of Solvent. We indicated above how Me_2SO and glycerol perturbed the interaction of magnesium with the *E conformation. This effect has profound implications in relation to P_i-derived phosphorylation, since only the *E conformation is considered to be P_i reactive. In fact, Figures 12 and 13 show that after preincubation with magnesium the substrate-reactive conformation was depleted. The finding that Me_2SO inhibited formation of the E?Mg species observed in its absence (Scheme V) implies that in the presence of Me_2SO all ATPase molecules are in the appropriate (*E) conformation for phosphorylation, irrespective of the magnesium concentration. The magnesium requirement of the phosphorylation process only reflects the fact that the $Mg{\cdot}P_i$ complex is the true substrate (Scheme II).

Scheme VI

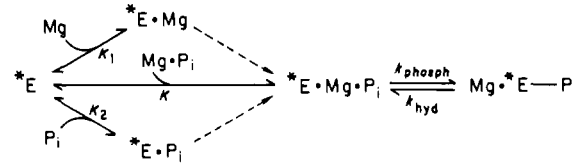

Conversely, in the absence of Me_2SO, the interaction of Ca^{2+}-deprived SR with Mg^{2+}, which *depletes* the P_i-reactive conformation of the ATPase, must be taken into account in the formulation of the reaction mechanism for enzyme phosphorylation, especially at neutral or slightly alkaline pH. Magnesium therefore has a dual effect on the phosphorylation reaction, since it allows formation of the true reaction substrate (the $Mg{\cdot}P_i$ complex) and simultaneously draws part of the ATPase away from the substrate-reactive conformation in a highly pH-dependent manner. Although Inesi et al. (1984) attempted to explain the pH dependence of the phosphorylation reaction by considering the various states of protonation of both the phosphate and different enzyme sites, assuming that all enzyme species were saturated with Mg^{2+}, we believe the role of magnesium must be given special attention, since ATPase–magnesium interactions did prove to be pH sensitive (Guillain et al., 1982, 1984). The following paragraphs show that this can be achieved by a straightforward modification of the conventional phosphorylation Scheme I.

Since $Mg{\cdot}P_i$ was found to be the substrate in the presence of Me_2SO, a logical first step toward elaboration of a new scheme was to start from Scheme I, which has been shown to account for *E-P measurements in the absence of solvent, and then tentatively introduce the $Mg{\cdot}P_i$ complex as a possible substrate in the absence of solvent as well, thus giving Scheme VI.

This scheme, which has *not* been examined previously (Kolassa et al., 1979), evidently leads to equilibrium *E-P values *identical* with those predictable from Scheme I, the only necessary relation being $K_2K_4 = K_1K_3 = KK_{ass}$, K being the affinity for $Mg{\cdot}P_i$ of the *E form and K_{ass} being the association constant for formation of the $Mg{\cdot}P_i$ complex. $Mg{\cdot}P_i$ may therefore be included in Scheme I as a possible substrate. The second step was to realize that measurement of equilibrium *E-P values does not even make it possible to ascertain whether all three species, Mg^{2+}, P_i, and $Mg{\cdot}P_i$, bind to the ATPase and produce the ternary complex or whether Mg^{2+} and P_i are competitive inhibitors for the $Mg{\cdot}P_i$ substrate binding (this is illustrated by dotted arrows in Scheme VI). Any set of equilibrium *E-P values compatible with Scheme I can therefore equally well be explained by assuming that $Mg{\cdot}P_i$ is the substrate and that Mg^{2+} and P_i behave as inhibitors [as previously noted, binding of $Mg{\cdot}P_i$ alone can of course not account for the measured phosphoenzyme levels (Kolassa et al., 1979; Inesi et al., 1984)].

On the other hand, we were able to design an experiment (Figures 12 and 13) that did demonstrate the inhibitory role of preincubation with magnesium. If we focus on the role of Mg^{2+}, Scheme VI then becomes Scheme III, in which Mg^{2+} is both a cosubstrate and a pH-dependent, Me_2SO-sensitive inhibitor. Scheme III is the simplest way to account for the fact that the maximal *E-P level is much lower at pH 7 than at pH 6 (Punzengruber et al., 1978; Beil et al., 1977; Inesi et al., 1984) and that it reaches a high pH-independent value in the presence of Me_2SO (de Meis et al., 1980).

Further Possible Refinement of Scheme III. We previously suggested that the $^*E \rightarrow E^?$ equilibrium was shifted by Michaelian binding of only *one* Mg^{2+} ion per two calcium sites (Guillain et al., 1982); in that case, Scheme III would only be able to account for a reduced $[^*E\text{-}P]_{max}$ but not for the drop in the $^*E\text{-}P$ level to zero experimentally observed at very high Mg^{2+} concentrations. The latter observation requires that the enzyme should somehow be able to carry at least two bound magnesium ions, as previously emphasized by Tanford's group (Loomis et al., 1982). This requirement can be satisfied by assuming that the substrate (i.e., $Mg{\cdot}P_i$) may also bind to the $E^?Mg$ enzyme, which is physically meaningful since the aspartyl site is of course also present in the $E^?$ conformation, although with an unknown affinity toward $Mg{\cdot}P_i$, and has in fact already been suggested (Loomis et al., 1982). We also have some preliminary evidence that free Mg^{2+} may even behave like a low-affinity competitor of $Mg{\cdot}P_i$ for binding to the ATPase catalytic site itself.

CONCLUSIONS

We have attempted to define here the mechanism of phosphoenzyme formation from P_i, at least in the absence of potassium, as comprising: (i) necessary cobinding at the catalytic site of Mg^{2+} and P_i ($Mg{\cdot}P_i$ binding) and (ii) one or several pH-dependent inhibitory effects of magnesium alone, at either the calcium or catalytic site. This composite scheme accounts for the apparent discrepancy between kinetic data and stoichiometry predictions, is consistent with previously published equilibrium data, and is further substantiated by the new kinetic experiments described in this paper. Lastly, we would like to make some purely speculative comments:

(i) Our proposed mechanism is in line with simple molecular representations, since the neutral substrate $Mg{\cdot}P_i$ can be expected to have easier access than charged substrates to the phosphorylation site of the $^*E$ (E_2) conformation, which has been suggested to be hydrophobic. This can also explain why the pump's apparent affinities for Mg^{2+} (a cation) and P_i (an anion) are relatively pH independent.

(ii) There is a qualitative difference between our proposal and the previously suggested random binding Scheme I, namely, that our suggestion *implies* that P_i and Mg^{2+} are both located inside the active site, whereas it is not necessarily a consequence of Scheme I. Consistent with this location of Mg^{2+} inside the catalytic site was the recent demonstration by Shigekawa et al. (1983) that in the forward mode of the calcium pump the metal component (M) of the nucleotide substrate remained bound to the enzyme until the phosphoenzyme $(M)E_2P$ (our $Mg{\cdot}^*E\text{-}P$) was hydrolyzed.

(iii) Two types of magnesium binding sites were found necessary to explain our data: the calcium binding site(s) and the metal/substrate binding site near the reactive aspartyl residue [there might be one or several tryptophans in the latter site, since simple nucleotide binding affects intrinsic fluorescence; see Dupont et al. (1982)]. Our interpretation does not require any other "specific" magnesium binding site. Recent work by Shigekawa et al. (1983) also points to the fact that there is no need to postulate any other divalent cation binding site except the substrate site and the transport site to account for the kinetics of ATP-derived phosphoenzyme hydrolysis.

ACKNOWLEDGMENTS

We thank Prof. P. D. Boyer and Kerstin E. Stempel (Molecular Biology Institute, University of California) for ^{18}O analysis and useful comments on the manuscript. The ^{18}O analysis was made possible by U.S. National Science Foundation Grant PCM-80-00817. We are also grateful to Pr. G. Inesi (University of Maryland Medical School, Baltimore, MD) for sending us one of his manuscripts prior to publication, to Pr. G. Hervé for stimulating discussions, and to Mathilde Dreyfus and Hélène Laborde for their help in editing and typing the manuscript.

Registry No. ATPase, 9000-83-3; P_i, 14265-44-2; Mg, 7439-95-4; Ca, 7440-70-2.

REFERENCES

Ariki, M., & Boyer, P. D. (1980) *Biochemistry 19*, 2001–2004.
Barrabin, H., Scofano, H. M., & Inesi, G. (1984) *Biochemistry 23*, 1542–1548.
Beil, F. U., Von Chak, D., & Hasselbach, W. (1977) *Eur. J. Biochem. 81*, 151–164.
Boyer, P. D., de Meis, L., Carvalho, M., & Hackney, D. D. (1977) *Biochemistry 16*, 136–140.
Carvalho-Alves, P. C., & Scofano, H. M. (1983) *J. Biol. Chem. 258*, 3134–3139.
Champeil, P., Büschlen, S., Bastide, F., & Gary-Bobo, C. M. (1978) *J. Biol. Chem. 253*, 1179–1186.
Champeil, P., Büschlen, S., & Guillain, F. (1981) *Biochemistry 20*, 1520–1524.
Champeil, P., Gingold, M. P., Guillain, F., & Inesi, G. (1983) *J. Biol. Chem. 258*, 4453–4458.
Cordone, L., Cupane, A., San Biagio, P. L., & Vitrano, E. (1979) *Biopolymers 18*, 1975–1988.
de Meis, L., & Vianna, A. L. (1979) *Annu. Rev. Biochem. 48*, 275–292.
de Meis, L., Martins, O. B., & Alves, E. L. (1980) *Biochemistry 19*, 4252–4261.
de Meis, L., de Souza Otero, A., Martins, O. B., Alves, E. W., Inesi, G., & Nakamoto, R. (1982) *J. Biol. Chem. 257*, 4993–4998.
Dreyfus, M., Vandenbunder, B., & Buc, H. (1978) *FEBS Lett. 95*, 185–189.
Dupont, Y. (1982) *Biochim. Biophys. Acta 688*, 75–87.
Dupont, Y., & Pougeois, R. (1983) *FEBS Lett. 156*, 93–98.
Dupont, Y., Bennett, N., & Lacapere, J. J. (1982) *Ann. N.Y. Acad. Sci. 402*, 569–572.
Epstein, M., Kuriki, Y., Biltonen, R., & Racker, E. (1980) *Biochemistry 19*, 5564–5568.
Guillain, F., & Boyer, P. D. (1982) *Ann. N.Y. Acad. Sci. 402*, 566–568.
Guillain, F., Gingold, M. P. Büschlen, S., & Champeil, P. (1980) *J. Biol. Chem. 255*, 2072–2076.
Guillain, F., Champeil, P., Lacapere, J. J., & Gingold, M. P. (1981) *J. Biol. Chem. 256*, 6140–6147.
Guillain, F., Gingold, M. P., & Champeil, P. (1982) *J. Biol. Chem. 257*, 7366–7371.
Guillain, F., Champeil, P., & Boyer, P. D. (1984) *Biochemistry 23*, 4754–4761.
Hackney, D. D., & Boyer, P. D. (1978) *Proc. Natl. Acad. Sci. U.S.A. 75*, 3133–3137.
Hackney, D. D., Stempel, K. E., & Boyer, P. D. (1980) *Methods Enzymol. 64*, 60–83.
Inesi, G., Kurzmack, M., Nakamoto, R., de Meis, L., & Bernhard, S. A. (1980) *J. Biol. Chem. 255*, 6040–6043.
Inesi, G., Watanabe, T., Coan, C., & Murphy, A. (1982) *Ann. N.Y. Acad. Sci. 402*, 515–534.
Inesi, G., Lewis, D., & Murphy, A. J. (1984) *J. Biol. Chem. 259*, 996–1003.
Kanazawa, T. (1975) *J. Biol. Chem. 250*, 113–119.
Kanazawa, T., & Boyer, P. D. (1973) *J. Biol. Chem. 248*, 3163–3172.
Knowles, A. F., & Racker, E. (1975) *J. Biol. Chem. 250*, 1949–1951.

Kolassa, N., Punzengruber, C., Suko, J., & Makinose, M. (1979) *FEBS Lett. 108*, 495-500.
Kuriki, Y., Halsey, J., Biltonen, R., & Racker, E. (1976) *Biochemistry 15*, 4956-4961.
Lacapere, J. J., Gingold, M. P., Champeil, P., & Guillain, F. (1981) *J. Biol. Chem. 256*, 2302-2306.
Loomis, C. R., Martin, D. W., McCaslin, D. R., & Tanford, C. (1982) *Biochemistry 21*, 151-156.
Marczek, Z., Nelson, R. W., Rosemblatt, M. S., & Ikemoto, N. (1983) *Biophys. J. 41*, 18a.
Makinose, M., & Hasselbach, W. (1971) *FEBS Lett. 12*, 271-272.
Martin, D. W., & Tanford, C. (1981) *Biochemistry 20*, 4597-4602.
Masuda, H., & de Meis, L. (1973) *Biochemistry 12*, 4581-4585.
McIntosh, D. B., & Boyer, P. D. (1983) *Biochemistry 22*, 2867-2875.
Punzengruber, C., Prager, R., Kolassa, N., Winkler, F., & Suko, J. (1978) *Eur. J. Biochem. 92*, 349-359.
Rauch, B., Von Chak, D., & Hasselbach, W. (1977) *Z. Naturforsch., C: Biosci. 32C*, 828-834.
Shigekawa, M., & Akowitz, A. A. (1979) *J. Biol. Chem. 254*, 4726-4730.
Shigekawa, M., Wakabayashi, S., & Nakamura, H. (1983) *J. Biol. Chem. 258*, 14157-14161.
The, R., & Hasselbach, W. (1977) *Eur. J. Biochem. 74*, 611-621.
Vianna, A. L. (1975) *Biochim. Biophys. Acta 410*, 389-406.
Watanabe, T., Lewis, D., Nakamoto, R., Kurzmack, M., Fronticelli, C., & Inesi, G. (1981) *Biochemistry 20*, 6617-6625.

Copper(I)-Bleomycin: Structurally Unique Complex That Mediates Oxidative DNA Strand Scission†

Guy M. Ehrenfeld, Luis O. Rodriguez,‡ and Sidney M. Hecht*

Departments of Chemistry and Biology, University of Virginia, Charlottesville, Virginia 22901

Cynthia Chang, Vladimir J. Basus, and Norman J. Oppenheimer*,§

Department of Pharmaceutical Chemistry, University of California, San Francisco, California 94143
Received May 30, 1984

ABSTRACT: Copper(I)-bleomycin [Cu(I)·BLM] was characterized in detail by ^{13}C and ^{1}H NMR. Unequivocal chemical shift assignments for Cu(I)·BLM and Cu(I)·BLM·CO were made by two-dimensional ^{1}H-^{13}C correlated spectroscopy and by utilizing the observation that Cu(I)·BLM was in rapid equilibrium with Cu(I) and metal-free bleomycin, such that individual resonances in the spectra of BLM and Cu(I)·BLM could be correlated. The binding of Cu(I) by bleomycin involves the β-aminoalaninamide and pyrimidinyl moieties, and possibly the imidazole, but not N^{α} of β-hydroxyhistidine. Although no DNA strand scission by Cu(II)·BLM could be demonstrated in the absence of dithiothreitol, in the presence of this reducing agent substantial degradation of [^{3}H]DNA was observed, as was strand scission of cccDNA. DNA degradation by Cu(I)·BLM was shown not to depend on contaminating Fe(II) and not to result in the formation of thymine propenal; the probable reason(s) for the lack of observed DNA degradation in earlier studies employing Cu(II)·BLM and dithiothreitol was (were) also identified. DNA strand scission was also noted under anaerobic conditions when Cu(II)·BLM and iodosobenzene were employed. If it is assumed that the mechanism of DNA degradation in this case is the same as that under aerobic conditions (i.e., with Cu(I)·BLM + O_2 in the presence of dithiothreitol), then Cu·BLM must be capable of functioning as a monooxygenase in its degradation of DNA.

The bleomycins are a structurally related group of antitumor antibiotics capable of inhibiting the growth of transformed cells in vitro and in vivo (Umezawa, 1971). Clinically, the bleomycins are employed for the treatment of squamous cell carcinomas and malignant lymphomas (Carter, 1978; Crooke, 1978; Umezawa, 1979). Interestingly, while the bleomycins are biosynthesized as copper chelates by *Streptomyces verticillus* (Umezawa et al., 1966), and both the Cu(II) and metal-free bleomycins can inhibit the growth of tumor cells in culture (Antholine et al., 1982; Ishizuka et al., 1967; Rao et al., 1980; Umezawa, 1971) and in experimental animals, the therapeutic effect mediated by bleomycin has been attributed to the ability of an Fe(II) complex of bleomycin to degrade DNA in an O_2-dependent transformation.

Umezawa and his co-workers have suggested that the activation of copper(II)-bleomycin (Cu(II)·BLM)[1] in situ involves initial conversion to Cu(I)·BLM; subsequent removal of Cu(I) by specific cellular metal binding proteins would then provide metal-free bleomycin, which could be transformed to the putative "active complex" following chelation of Fe(II)

† This work was supported at the University of Virginia by National Institutes of Health Research Grants CA-27603 and CA-29235 and at the University of California by National Resonance Laboratory Research Resource Center Grants NSF-GP-23633 and NIH-RR-00711.

‡ Fellow of the Economic Development Administration of Puerto Rico. This study was carried out as part of the doctoral program in absentia from Massachusetts Institute of Technology.

§ National Institutes of Health Research Career Development Awardee, 1979-1984.

[1] Abbreviations: BLM, bleomycin; TCA, trichloroacetic acid; 2-D, two dimensional; Me_2SO, dimethyl sulfoxide; CO, carbon monoxide; Me_4Si, tetramethylsilane; EDTA, ethylenediaminetetraacetic acid; Tris, tris(hydroxymethyl)aminomethane.

0006-2960/85/0424-0081$01.50/0